Monomer-Polymer Equilibria in the Axon: Direct Measurement of Tubulin and Actin as Polymer and Monomer in Axoplasm

JAMES R. MORRIS and RAYMOND J. LASEK
Department of Anatomy, Case Western Reserve University, School of Medicine, Cleveland, Ohio 44106; and Marine Biological Laboratory, Woods Hole, Massachusetts 02543

ABSTRACT The monomer-polymer equilibria for tubulin and actin were analyzed for the cytoskeleton of the squid giant axon. Two methods were evaluated for measuring the concentrations of monomer, soluble (equilibrium) polymer, and stable polymer in extruded axoplasm. One method, the Kinetic Equilibration Paradigm (KEP), employs the basic principles of diffusion to distinguish freely diffusible monomer from proteins that are present in the form of polymer. The other method is pharmacological and employs either taxol or phalloidin to stabilize the microtubules and microfilaments, respectively. The results of the two methods agree and demonstrate that 22–36% of the tubulin and 41–47% of the actin are monomeric. The in vivo concentration of monomeric actin and tubulin were two to three times higher than the concentration required to polymerize these proteins in vitro, suggesting that assembly of these proteins is regulated by additional mechanisms in the axon. A significant fraction of the polymerized actin and tubulin in the axoplasm was stable microtubules and microfilaments, which suggests that the dissociation reaction is blocked at both ends of these polymers. These results are discussed in relationship to the axonal transport of the cytoskeleton and with regard to the ability of axons to change their shape in response to environmental stimuli.

Cytoskeletal Dynamics

Linear cytoskeletal polymers, such as microtubules (MT)[1] and microfilaments (MF), provide the framework of cytoskeletons. These cytoskeletal elements are part of a larger cytoskeletal system that includes the subunits in the free monomer pool. There is a continuous flux of subunits between the polymers of the cytoskeleton and the monomer pool (19, 22, 32). This makes the cytoskeletal system dynamically responsive and large changes in the state of the system can occur when the monomer-polymer equilibrium is altered. The chemistry of polymer assembly and disassembly is simplified by the fact that only the ends of the polymers are reactive (16, 22, 40, 55). Thus, the kinetics of assembly and disassembly can be effectively described by a few rate constants for the association and dissociation reactions at the ends of the polymers (16, 40, 55). These reactions differ at each end of the polymer and each association and dissociation reaction can be separately regulated.

The assembly or disassembly reactions may be blocked at one or both ends of a polymer. If the disassembly reactions at both ends are blocked, the polymer will be stable and will not disassemble when the monomer concentration is reduced (22, 40, 55). These "stable polymers" differ markedly from those polymers that have active dissociation reactions at one or both ends. This latter group of polymers can be considered "equilibrium polymers" because they are in equilibrium with the monomer pool (16, 22). Equilibrium polymers are responsive to changes in the concentration of monomer and decrease in length if the monomer concentration declines (22, 40, 55). Cytoskeletons are a mixture of stable polymers and equilibrium polymers (5, 32, 51). The responsive properties of a cytoskeletal system are influenced by the balance between these different types of polymers.

In most cells, the cytoskeleton can be treated as a single system that is interconnected through the free monomer pool.

[1] *Abbreviations used in this paper:* KEP, Kinetic Equilibrium Paradigm; MT, microtubules; MF, microfilaments.

THE JOURNAL OF CELL BIOLOGY · VOLUME 98 JUNE 1984 2064-2076

The equilibration rate between two regions of the monomer pool is principally determined by the diffusion rate and the distance between the regions in question. Diffusion is a rapid process over the range of a few tens of microns, which encompasses most cells. In large cells such as neurons the distances may be so great that diffusion becomes a limiting factor in the equilibration between spatially separated regions of the monomer pool. However, diffusion is sufficient to integrate the activities of the cytoskeleton between different parts of most cells and within circumscribed regions of large cells.

Monomer-Polymer Equilibria in Cells

The dynamic state of a cytoskeletal system can be rigorously defined by two sets of parameters: (*a*) the concentration of reactants, which include the amount of polymerized protein and the concentration of subunits in the monomer pool, and (*b*) the rate constants for the assembly-disassembly reactions. Although these parameters are not all readily measured in living cells, a useful approximation of the dynamic state of a cytoskeletal system can be obtained by measuring the monomer-polymer ratio.

The monomer-polymer ratio can be used to compare the steady state conditions between two different types of cells or within the same cell that is undergoing cytoskeletal reorganization. For example, the monomer-polymer ratio for tubulin and MT changes when the cytoskeleton is reorganized during mitosis, cell movements, morphogenesis, and secretion (1, 5, 6, 10, 19, 39, 42, 45, 51). The monomer-polymer ratio of actin and MF also usefully reflects the dynamics of this component of the cytoskeleton (2, 10, 41, 44). Thus, measurements of the concentration of monomer and polymer in a cell can provide physiologically relevant information about the reaction kinetics that are involved in cytoskeletal organization.

Monomer-Polymer Measurements in Differentiated Cells

With few exceptions (42, 43), most of the information about the regulation of polymerization in intact cells has been derived from cells in culture. Cultured cells have been chosen for such studies because homogeneous, synchronized populations of cells can be obtained that are essentially all in the same physiological state. It would be valuable to have comparable information for more fully differentiated cells such as those in the nervous system. However, measurements of total monomer and polymer concentration from a structure as complex as the brain have a limited value because the sample includes an incredible variety of cells. In a few special cases, individual cells or their processes can be dissected from the nervous system. In this regard, the squid giant axon is a particularly favorable preparation for analyzing cytoskeletal dynamics. Axoplasm can be easily separated from the plasma membrane of the squid giant axon without significantly disturbing cytoskeletal organization or axoplasmic function (4). Axons have the additional advantage that their cytoskeletons are relatively homogeneous. We have utilized these special features to develop a new method of measuring the amount of free monomer and polymer in this specialized region of a fully differentiated neuron.

Kinetic Equilibration Paradigm

Our method is based on the fact that axoplasm extruded from the giant axon is a uniform cylinder that retains its shape in physiological buffers for many hours (35). To measure the amount of monomer and polymer in the axoplasm, the cylinder of axoplasm is placed into a volume of buffer. Under these conditions, the relationship between the physical state of the proteins and the rate at which proteins elute from the axoplasmic cylinder can be observed. For example, monomeric proteins that are free to diffuse within the axoplasm will enter the surrounding buffer at a rate that is determined both by the diffusion constant of the protein and by the geometry of the cylinder. On the other hand, polymerized proteins will enter the surrounding buffer at a slow rate that is principally determined by the disassembly reaction from the ends of the polymer. Fig. 1 illustrates the predicted behavior of such a model system, which is termed the Kinetic Equilibration Paradigm (KEP). (See figure legend and results for more details.)

In this paper the usefulness of the KEP for measuring the amounts of tubulin and actin that are in the form of monomer, soluble polymer, (equilibrium polymer), and stable

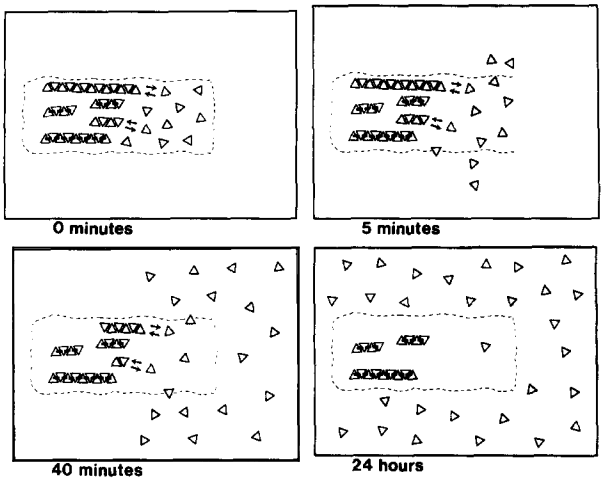

FIGURE 1 The kinetic equilibration paradigm (KEP). The panel on the upper left shows a sample of axoplasm (containing stable polymers, soluble polymers, and monomers) immediately after extrusion into a large buffer bath. The arrows indicate sites of monomer-polymer exchange on soluble polymers (equilibrium polymers). The next panel on the upper right, shows monomeric protein diffusing into the buffer 5 min after extrusion. Next (*bottom left*), by 40 min most of the monomeric protein has eluted and soluble polymers have begun to depolymerize due to the low concentration of monomer. Finally, by 2 h, essentially all of the soluble protein has eluted and only the stable polymers remain in the axoplasmic ghost.

Elution is initiated by placing a cylinder of axoplasm into a defined buffer. Subunits that are free to diffuse will rapidly elute from the axoplasm into the buffer during the first few minutes. As the monomer concentration in the axoplasm falls, the polymers that are in equilibrium with monomer will depolymerize. If the rate of diffusion is relatively rapid compared with the rate of polymer disassembly, then most of the cytoskeletal protein entering the extraction medium will represent the disassembly of polymers that are in equilibrium with the monomer pool. We will use the operational term soluble polymers to refer to the polymers that depolymerize when the monomer concentration is reduced, $\Delta\nabla\Delta\nabla$, stable polymer; $\nabla\Delta\nabla\Delta$, soluble polymer; Δ, diffusible monomer.

polymer is evaluated. The results of the KEP are compared with those obtained by a pharmacological method for measuring monomer-polymer ratio. This latter method employs either taxol and phalloidin to selectively stabilize either MT or MF, respectively (50, 57). The results of the two methods agree and suggest that a large amount of monomer is available locally in the axon for the polymerization of additional MT and MF. These reserves may be important in the ability of the axon to undergo local changes in its cytoskeletal organization.

MATERIALS AND METHODS

Isolation of Axoplasm: Squid (*Loligo pealii*) were supplied by the Marine Biological Laboratory in Woods Hole, MA and were used in these experiments 48 hr after their capture at sea. Axoplasm was obtained using a modification of the procedure described by Lasek, which has been described in detail elsewhere (26). When the axoplasm is extruded it apparently yields under pressure at a plane that is between 0.3–10 μm deep to the plasma membrane (R. J. Lasek, K. Fath, and S. T. Brady, unpublished observation). This explains why extruded axoplasm emerges as a cylinder and a thin layer of axoplasm remains associated with the plasma membrane.

Buffer P: Buffer P was designed to carefully simulate the solution conditions in the squid giant axon. It contains various amino acids, organic metabolites, carbohydrates, inorganic ions, ATP, and GTP at their reported physiologic concentrations (8, 9). The composition of buffer P is detailed elsewhere (35). EGTA and phenylmethylsulfonyl fluoride were included in buffer P to chelate Ca^{2+} and inhibit proteolysis, respectively. It is important to note that axoplasm contains ~2% protein (see Results and reference 18). Buffer P was assembled from refrigerated or frozen stock solutions, brought to room temperature, and millipore-filtered immediately before use.

SDS PAGE: The SDS PAGE system used in these experiments were described elsewhere (35). The gels were stained with Coomassie Blue. Densitometric analysis was performed by scanning gel lanes at 600 nm on a Feiss M4Q III scanning densitometer. The areas under absorbance peaks representing proteins of interest were measured using a Numonics model 1224 electronic digitizer (Numonics Corp., Landsdale, PA).

Incubation of the Giant Axon in [^{3}H]Leucine: A cleaned giant axon was incubated for 2 h in 0.5 ml of artificial sea water without Ca^{++}-containing [^{3}H]leucine (1 mCi/ml) using a method described elsewhere (26). Artificial sea water with Ca^{++} contained 425 nM NaCl, 9 nM KCl, and 50 nM EGTA (pH 7.6).

Agarose Cylinders for Modeling Experiments: Experiments to model diffusion in axoplasm were conducted using agarose cylinders because this medium had been shown to be very effective in similar studies (12). The cylinders contained 1% agarose (Sigma Chemical Co., St. Louis, MO) and were equilibrated in ^{125}I, which was the diffusant. The cylinders were constructed as follows:

Agarose was dissolved in deionized water. ^{125}I (New England Nuclear, Boston, model no. NEZ-033) was added to the agarose solution at a concentration of 50 μCi/ml. Samples of this solution were then drawn into 100-μl micropipets (Fisher Scientific Co., Pittsburgh, PA, model no. 21-164-2H) and allowed to gel. Immediately after gelation had occurred the cylinders were expelled into a plastic petri dish where they were stored in a humid environment prior to use. The cylinders that were produced in this manner were 1.6-mm diam and cut to uniform lengths of 1 cm for experimental use.

Drug Stabilization Experiments: Several experiments were performed to examine the solubilities of axoplasmic cytoskeletal proteins in the presence of drugs that are known to stabilize cytoskeletal polymers. Taxol (a microtubule-stabilizing agent) was generously donated to this study by the National Cancer Institute's Drug Synthesis and Chemistry Branch. Taxol is purified from the plant *Taxus brevifolia* and is used as an antimitotic chemotherapeutic agent (49). For use in these experiments, a 10-mM stock solution of taxol in dimethyl sulfoxide was made and diluted to 10-μM concentration in buffer P prior to use.

In a second series of experiments, phalloidin was used because of its ability to stabilize actin containing MF (30). Phalloidin was obtained from Boehringer Mannheim Biochemicals (No. 166 049); Indianapolis, IN. A 10-mM stock solution of phalloidin was made up in dimethyl sulfoxide and diluted to 10-μM concentration in buffer P prior to use. Control experiments were performed using buffer P with 0.1% dimethyl sulfoxide.

RESULTS

Measurements of Axoplasmic Protein Concentration

The following analysis relies upon our ability to accurately determine protein concentration by measuring the optical density of Coomassie Blue-stained proteins in SDS polyacrylamide gels. To define the accuracy of this method, several concentrations of a standard protein (BSA) were run on our SDS PAGE system, stained with Coomassie Blue, and scanned with a densitometer at 600 nm (Fig. 2). This analysis showed a linear response (correlation coefficient = 0.999) over a range from 0.5 to 10 μg of protein (Fig. 3). Consequently, all further densitometric analyses were performed at protein concentrations within this range. When several con-

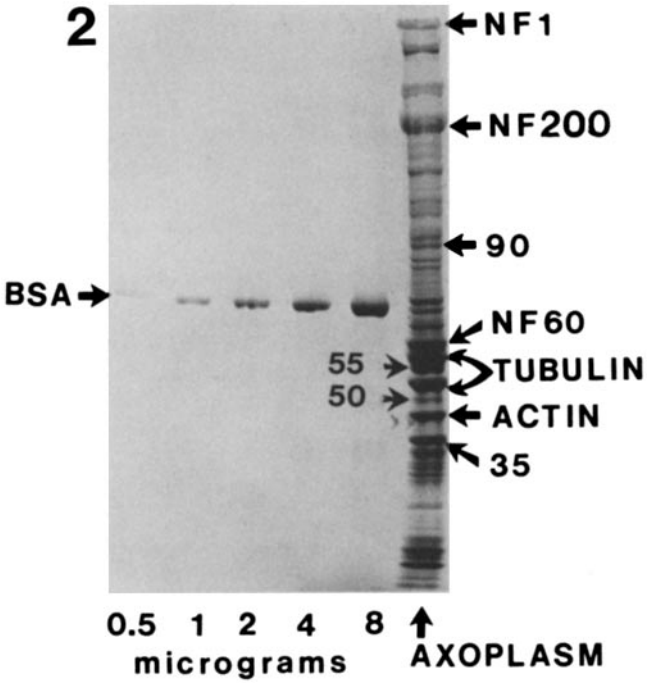

FIGURE 2 BSA standard and axoplasmic proteins. This polyacrylamide gel illustrates the staining properties of various amounts of BSA and shows the Coomassie Blue staining pattern of the proteins in axoplasm. Gels similar to this were used to measure protein mass in this study. It is clear that actin, tubulin, and the neurofilament proteins (*NF1*, *NF200*, and *NF60*) are present in large amounts in axoplasm. Other proteins, which are discussed in the text are also labeled. Values *90*, *55*, *50*, and *35* represent molecular weight × 10^{-3}.

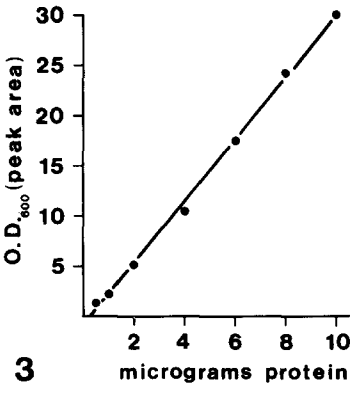

FIGURE 3 Linear gel densitometry. This graph shows that the densitometric response using Coomassie Blue is linear over the range of protein mass (0.5–10 μg) used in this study.

centrations of whole axoplasm were subjected to a similar analysis a linear response was also obtained for a number of the major proteins, indicating that Coomassie Blue stains both BSA and axoplasmic proteins with similar stoichiometry.

Next, the curve relating protein mass to optical density for BSA (Fig. 2) was used as a standard to determine the concentration of protein in axoplasm. This analysis showed that axoplasm contains 25 mg/ml (2.5%) protein. This result is similar to the reported value for squid axoplasm (2%) as measured by both gravimetric and Lowry methods and offers further support for the accuracy of our densitometric analysis (18). The concentrations of several major axoplasmic proteins (neurofilament protein, tubulin, actin, and proteins at 35 and 90 k daltons) were also determined. The results of these measurements are listed in Table I. These values will be used later in our data analysis to determine the mass concentrations of tubulin and actin which are polymerized or monomeric in axoplasm.

Development of the Kinetic Equilibration Paradigm to Study Molecular Diffusion

One method, which may be used to assay diffusion in a body such as a cylinder, is to measure the rate at which a substance elutes from the cylinder into the surrounding medium. If the concentration in the medium is kept very low, then the elution kinetics describe the mobility of the substance in the cylinder. We call this type of analysis the Kinetic Equilibration Paradigm (KEP), because the concentration of the diffusible substances in the cylinder tends to equilibrate with that in the medium. The physical theory for the equilibration of a cylinder is well established (15, 24). For a brief description of the equation that models this system and the relevant parameters, see Appendix A.

To test the validity of our particular experimental conditions, we analyzed the elution of a small diffusible molecule (^{125}I) from 1% agarose cylinders with dimensions similar to that of axoplasm extruded from the giant axon. Several baseline conditions must be met for this method to achieve success. First, a low concentration of diffusant in the environment must be maintained to minimize any return of diffusant into the cylinder during the experiment. Second, the extraction bath should be well mixed to avoid the formation of concentration gradients along the surface of the cylinder. Third, the cylinder should be long relative to its diameter to minimize effects due to the variation of geometry at its ends.

TABLE I

Protein Composition of Axoplasm

Protein	Fraction (1%) of axoplasmic protein	Concentration
		mg/ml
Tubulin (a + b)	22	5.6
Neurofilament (NF1 + NF200 + NF60)	13	3.3
Actin	6	1.4
35-kdalton protein	6	1.4
90-kdalton protein	1	0.2
Others	48	12.2
Total	100	24.1 (2.4%)

These conditions were tested by placing an [^{125}I]agarose cylinder in a relatively large (5 ml) single bath of deionized water. The cylinders were 6 μl in volume and similar in diameter to an axoplasmic cylinder (eg., 0.5 mm). Ideal mixing was approximated by constantly stirring the bath with either the tips of a pair of forceps or a micro-magnetic stirrer. Samples were taken from the bath at several times during the equilibration of ^{125}I. The radioactivity in each sample was measured and the concentration of ^{125}I in the bath was determined over time. These measurements were compared with an experiment in which an agarose cylinder was transferred through several well mixed smaller baths (0.5 ml) during the elution of ^{125}I. In this version of the KEP, each bath contains the fraction of ^{125}I which eluted during the time that the agarose cylinder was in that bath. This transfer protocol maintains a low concentration of diffusant because each bath is several orders of magnitude larger in volume than the cylinder and because the cylinder is repeatedly transferred to a fresh bath. The elution profiles that resulted from these two methods were indistinguishable, demonstrating that both the single bath and the transfer protocols are equivalent. This result also demonstrates that little of the eluted ^{125}I is carried on the surface of the agarose cylinder as it is transferred from bath to bath. The results obtained for the elution of ^{125}I from the agarose cylinders were identical to the calculated rate of elution predicted by diffusion theory. These results are not shown to conserve space but were similar to those for the elution of [^{3}H]leucine from axoplasm illustrated in Fig. 4.

Measurements of Amino Acid Diffusion in Axoplasm

The ability of the KEP to follow diffusion of a small molecule in axoplasm was then tested using [^{3}H]leucine as the diffusant. We employed leucine as the diffusant because the kinetics of uptake into the intact axon have previously been defined. Amino acids are not converted into macromolecules by axoplasm. An intact giant axon was equilibrated in a bath of artificial sea water containing [^{3}H]leucine as previously described (26). The axoplasm was extruded and transferred through several baths of buffer P. Fig. 4 shows the elution data for two different samples of axoplasm co-plotted

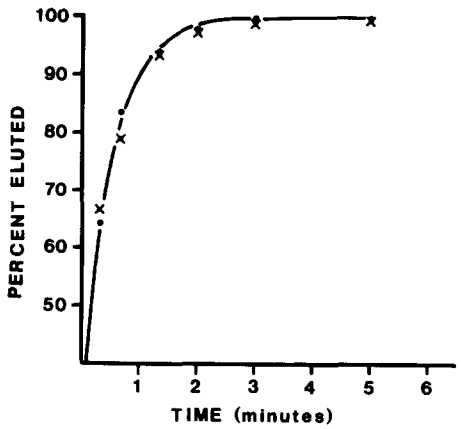

FIGURE 4 [^{3}H]leucine elution kinetics from axoplasm. This figure illustrates a comparison of data (dots, axon 1 and crosses, axon 2) obtained using two samples of axoplasm and the theoretical predictions (870-μm diam) for the elution of an amino acid from a cylinder of axoplasm. See Appendix I for a description of the theoretical analysis.

with the theoretical curve for the equilibration of leucine by diffusion. According to theory, the elution of an amino acid has a half time of ~20 s from a cylinder the size of extruded axoplasm. The data fall along the theoretical curve, indicating that leucine is freely diffusible in axoplasm. The small variation in results between samples of axoplasm can be accounted by errors in sampling, timing, and variations in the geometry of extruded axoplasm. We conclude that the KEP can be successfully applied to measure the diffusion of molecules from axoplasm into buffer P using a transfer protocol.

Equilibration of Axoplasmic Proteins with the Bath

Next, the transfer protocol was used to measure the equilibration of intrinsic axoplasmic proteins. This protocol included transfers through nine 0.5-ml baths. The transfer times were at 1, 2, 4, 8, 16, 30, 50, 80, and 120 min after extrusion. These transfer times were selected to allow a detailed comparison of elution at both early and late times and at the same time, maximize the amount of protein collected in each bath. The experiment was terminated at 120 min because our previous analysis of the axoplasmic ghost showed that all of the soluble proteins are extracted from axoplasm by this time (35).

At the conclusion of this transfer experiment each bath was sampled and prepared for SDS PAGE. Fig. 5 shows a typical gel pattern that resulted from this protocol. It is clear that the soluble proteins do not elute from axoplasm at rates that are proportional to their monomeric molecular weight, as theory would predict. For example, the protein labeled *90* has ceased elution by 50 min, whereas actin (at 43-kdaltons) is still eluting at later times. It is also clear that a small amount of NF protein (NF 200 and NF 60) appears in the later baths. This probably results from mechanical damage sustained by the axoplasm as it is transferred between baths because when axoplasm is extracted in a single bath no NF protein is soluble. (35). We noted that the axoplasm became more fragile toward the end of the experiment and small pieces were found in the bath. This had very little effect in the kinetic measurements as we will show later.

Quantitation of the Proteins Eluting from Axoplasm

Gels such as that shown in Fig. 5 were subjected to quantitative analysis by densitometric scanning. We were able to employ 1D-PAGE for this analysis because of the relative simplicity of the major protein composition of the axoplasm. The primary problem with this approach is the possibility of hidden proteins that have the same molecular weight as the proteins chosen for analysis. This was unlikely in the case of the cytoskeletal proteins of the axoplasm because these proteins so completely dominate the axoplasmic composition. This is documented by separating the axoplasmic proteins using 2D PAGE (Fig. 7). In this experiment the gel was purposefully overloaded to bring out contaminating proteins. No proteins appeared on the 2D PAGE that were not resolved by 1D PAGE. That is, there were no hidden bands on the 1D gels.

Fig. 6 illustrates examples of typical densitometric scans that were obtained from the Coomassie Blue-stained 1D gels. The baseline declines gradually from the low molecular weight

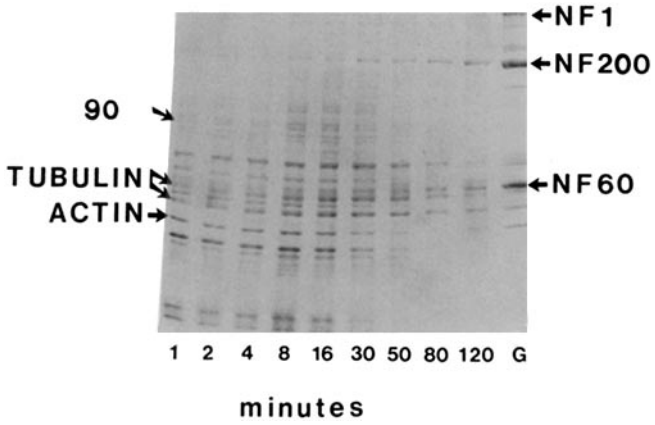

FIGURE 5 SDS page of protein elution kinetics using a single axon. This figure shows one of the gels used in the analysis of protein elution from a single sample of axoplasm. It is clear that protein elution in not simply related to monomeric molecular weight because all proteins of similar molecular weight do not elute at similar rates. Note that only a fraction of the axoplasmic ghost was loaded in the gel to avoid overloading the column with neurofilament protein.

end of the gel toward the high molecular weight end. This gradual change in optical density reflects the gradient of acrylamide in our gel system. Most of the major bands were well separated from each other on the 1D gels (Fig. 5). Two proteins (55 and 50 kdaltons), which can be seen clearly on the 2D gel in Fig. 7, ran near the tubulin peaks. The 50-kdalton protein was a minor peak and was insignificant in the analysis. The 55-kdalton protein which was located between alpha and beta tubulin ran closer to alpha tubulin than to beta tubulin on the 1D gels (Fig. 6). To control for the effects of this protein on the quantitation of tubulin, we compared the relative quantities of the individual alpha and beta tubulin subunits in each experiment. The results were the same for the different tubulin subunits in all cases. This observation indicates that the quantitative analysis of alpha tubulin was not significantly affected by the 55-kdalton protein. This is not surprising because the 55-kdalton bands and alpha tubulin can be distinguished as separate peaks (Fig. 5) so that only a relatively small portion of the 55-kdalton protein peak contributes to the alpha tubulin peak.

The Single Axon KEP

Quantitative data for the elution of tubulin and actin from individual axoplasm cylinders is illustrated in Fig. 8, *a* and *b*. The shaded region represents the 95% confidence envelope for the data means (filled circles) whereas the dashed lines represent diffusion theory kinetics for proteins of similar molecular weight and shape (see Appendix I). It is clear that both tubulin and actin elute from axoplasm more slowly than predicted for the free diffusion of monomeric protein. Because of the low standard error between samples, the following analysis of these results was carried out using the data from individual samples of axoplasm.

To determine if the elution of tubulin and actin could be explained by a simple exponential process (like diffusion) the data was replotted on semi-log axes. Because diffusion theory predicts an exponential time course of elution (see Appendix I), any process superimposed upon diffusion should cause the

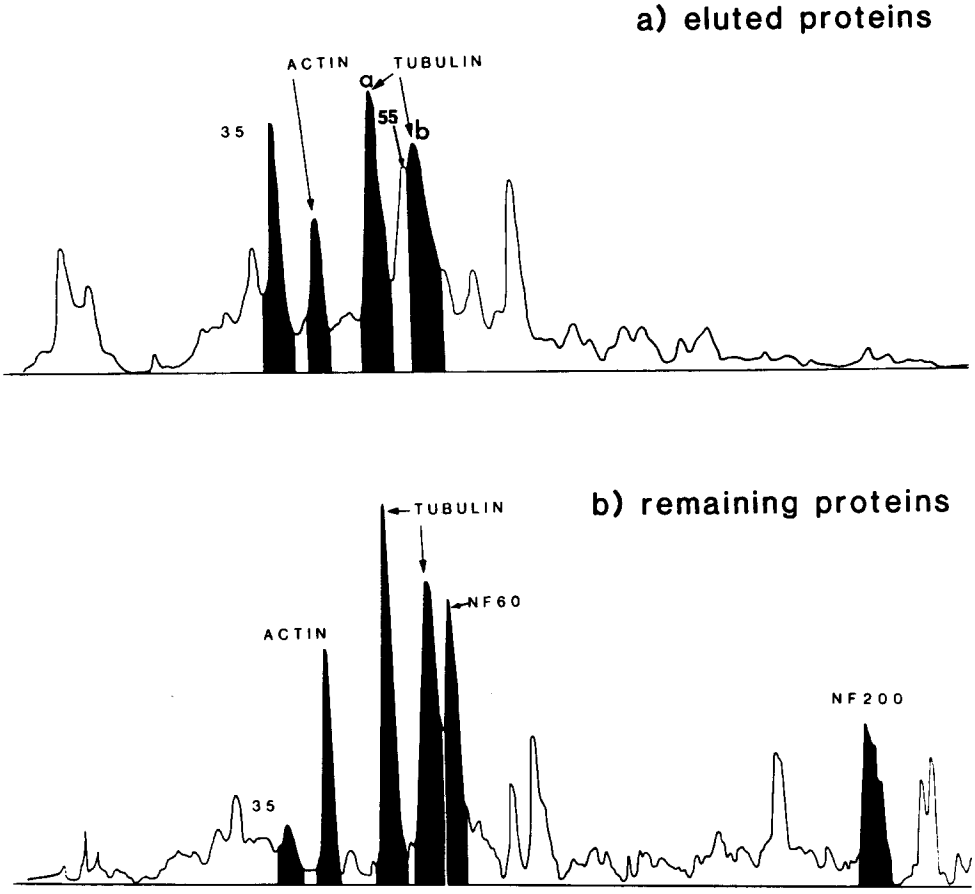

FIGURE 6 Densitometric scans of two typical samples from an elution experiment. This figure contains two densitometric scans showing the proteins eluted from axoplasm (*a*) and those proteins remaining in axoplasm (*b*) during an extraction experiment. Scans like these were used in quantitative analyses by first drawing a "baseline" that connects the lowest response points in the scan. This baseline identifies the background level of absorbance in the polyacrylamide gel. The selection of the baseline points agreed with the gels in every case. Then, peaks interest were selected (also using the actual gel as a guide) and perpendiculars were dropped from valleys on both sides of the peak. The areas defined, which are filled in for this figure, were measured using either gravimetric methods or digitization planimetry (both methods gave the same results).

data to deviate from a straight line when it is plotted in this manner. Fig. 8, *c* and *d* show the elution data for tubulin and actin from representative samples of axoplasm. Similar curves were obtained in all experiments (for tubulin $n = 4$; actin $n = 5$). It is clear that the data (filled circles) do not fall along a single line. Instead, the elution of tubulin and actin can be modeled as the sum of two exponential components. That is, there is an early, rapid efflux of protein that lasts until 10–20 min after extrusion and then a more slowly eluting form becomes predominant. It is important to note that this biphasic curve was not an artifact of this model, because the low molecular weight substances eluted with monophasic kinetics except for the last few percent of the material. Thus, the biphasic kinetics were not a general property of elution from the axoplasmic cylinders, and appear to be a special property of the proteins.

This type of equilibration curve is typical of two-component systems as described in the field of compartmentation analysis (47). The data become linear at long times because only one exponential term survives for large values of time. The two exponential components revealed in the semi-log plot may be extracted from the data using the method of exponential peeling (47). Briefly, linear regression analysis is used to find the best fit (maximized correlation coefficient) line for the data taken at longer times. This line is extrapolated to earlier times and subtracted from data that was not used in the regression analysis. The resulting values represent the fraction of soluble protein that elutes in the first component. This process was repeated for the tubulin and actin eluting from each sample of axoplasm. Fig. 8, *c* and *d* show the representative curves after this analysis. The solid line is the linear regression line for the second component and the dashed line represents the "peeled" first component. The slopes of the first and second components differ by as much as an order of magnitude. The "peeled" first component in each case is linear (correlation coefficient = 0.999) and elutes at a rate that is similar to that predicted by diffusion theory. These results support the idea that the first component represents an exponential process that can be accounted for by diffusion of either tubulin or actin.

The semi-log plot may be used to measure the fraction of tubulin or actin in axoplasm that contributes to each component. This is done by extrapolating the regression line for the second component to zero time, where it intersects the ordinate axis. The value at the point of intersection (I_{DP}) represents a measure of the fraction of soluble protein that contributes to the second component at the time of extrusion. The values of I_{DP} for tubulin and actin are 69 and 35.4%, respectively, in the examples shown in Figs. 8, *c* and *d*. The difference between this value and 100% is a measure of the fraction of soluble protein that contributes to the first component. These values were measured for the tubulin and actin in each sample of axoplasm. The resulting values were then used to calculate the fraction of total axoplasmic tubulin and actin in each component by taking into account the insoluble (stable) fraction of these proteins (35). Using the values for the concentrations (as milligrams per milliliter) of tubulin and actin in whole axoplasm, the concentrations of these proteins as stable polymer, soluble polymer (second component), and monomer (first component) were calculated. These data are displayed in Table II for tubulin and Table III for actin next to the heading "Single Axon KEP."

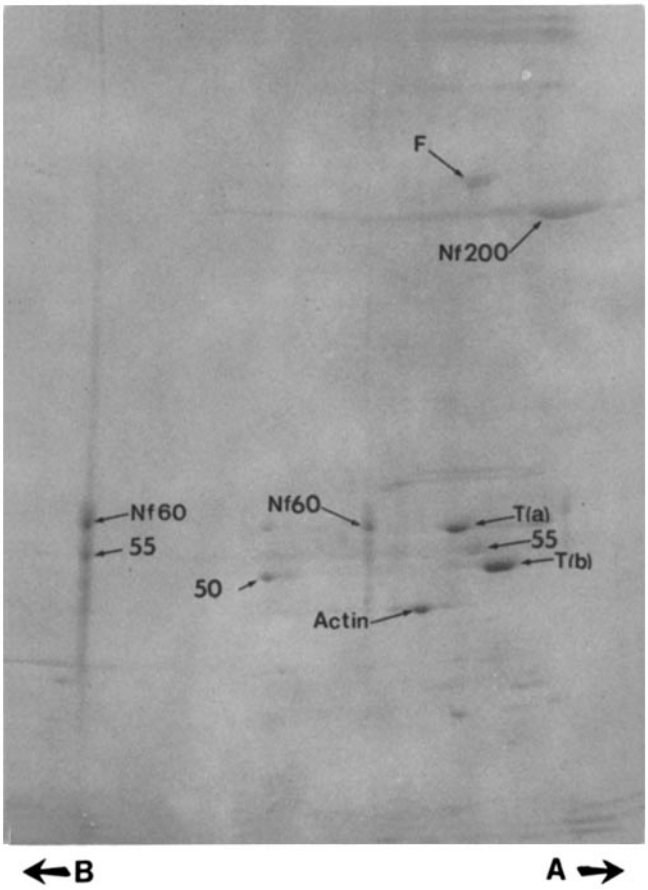

FIGURE 7 Two dimensional polyacrylamide gel electrophoresis of axoplasmic proteins. This figure illustrates the pattern of proteins from whole axoplasm obtained by 2D SDS PAGE. Several of the major proteins of interest are labeled on the gel including alpha tubulin (*Ta*), beta tubulin (*Tb*), the neurofilament proteins (*Nf200* and *Nf60*), and fodrin (*F*). Other bands that can not be associated with characterized proteins are designated by their nominal molecular weight. Note that some of the Nf60 and 55-kdalton protein run anomalously as a streak on the basic side of the gel. This probably represents an artifact of overloading the proteins that produces complexes during the isoelectric focusing step. This gel demonstrates that the protein composition of axoplasm is relatively simple and that no two proteins have exactly the same molecular weight. That is, there do not appear to be any hidden bands on the ID gels (Figs. 2, 5, and 6).

Ratio Analysis of Protein Equilibration—The Ratio KEP

It is difficult to use single axons to generate the entire series of protein equilibration kinetics because of the small amounts of protein in each sample and the increasing fragility of the axoplasm as it is handled frequently during transfers from bath to bath. To avoid these difficulties an alternative method was developed to obtain elution profiles for tubulin and actin. In this analysis, single samples of axoplasm were used to obtain the fraction of soluble protein that had eluted over a single interval of time. A sample of axoplasm was extruded into a large (1 ml), well-mixed bath of buffer P. The axoplasm was extracted for a measured time, removed from the bath with forceps, homogenized in a solubilizing solution containing mercaptoethanol and SDS (35), and analyzed by SDS PAGE. An aliquot of the extraction bath was also collected

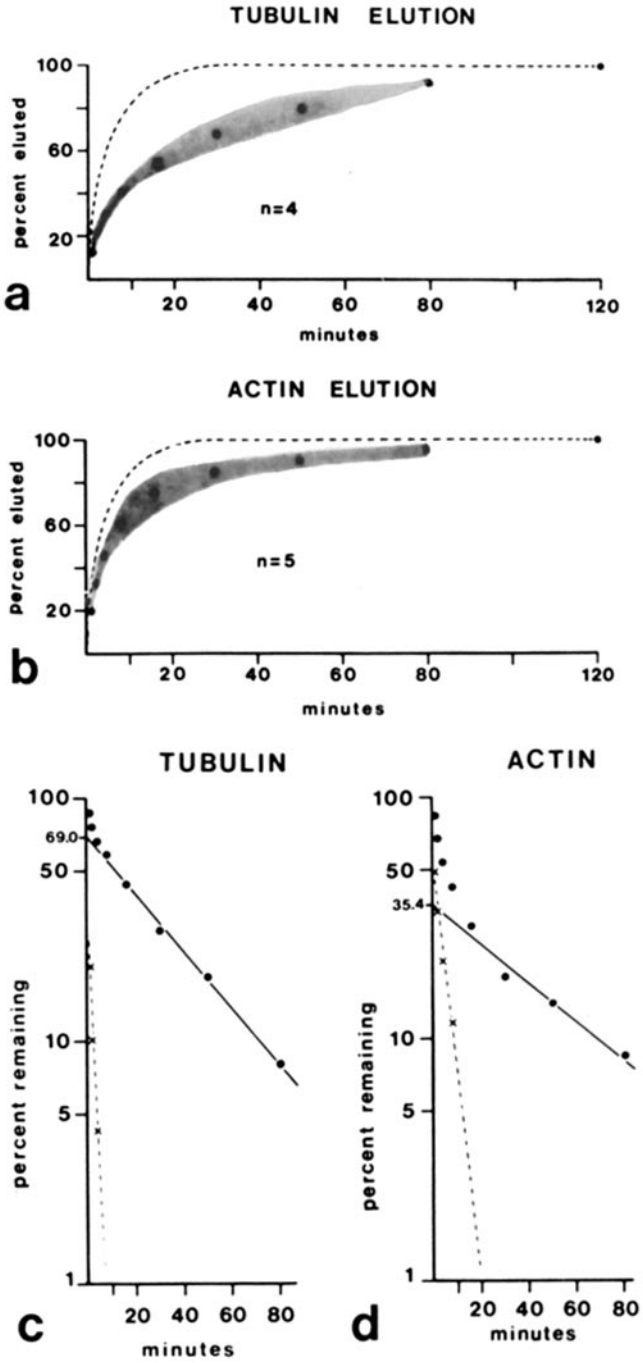

FIGURE 8 (*a* and *b*) Single axon KEP-elution profiles of tubulin and actin on cartesian axes. This figure shows the averaged data (filled circles) for the elution of tubulin and actin from axoplasm. The shaded regions represent the 95% confidence envelopes for the data and *n* indicates the number of axons used. The dashed line represents the elution profile predicted by theory for the diffusion of monomeric protein. It is clear than tubulin and actin elute more slowly than predicted for monomer. (*c* and *d*) Single axon KEP-elution profiles of tubulin and actin on Semilog axes. This figure illustrates representative elution data obtained from a single sample of axoplasm. The data (filled circles) was plotted on semi-log axes to determine if it could be described by a function of one exponential. Because the data is clearly nonlinear, a model function consisting of a sum of two exponentials was fit to the data using the method of exponential peeling (47). The crosses represent the more rapidly eluting fraction of tubulin and actin. This fraction elutes at a rate that is similar to theoretical predictions for monomeric diffusion.

TABLE II

Concentration of Each Form of Tubulin in Axoplasm

	Stable polymer*	Soluble polymer*	Monomer*	*n*
Single axon kinetics	15. ± 1.3 (0.84)	58.8 ± 2.9 (3.29)	26.2 ± 2.9 (1.47)	4
Ratio kinetics	17.6 ± 2.1 (0.99)	59.7 (3.35)	22.7 (1.27)	5
Taxol treatment	17. ± 2.9 (0.95)	46.5 ± 1.8 (2.6)	36.5 ± 3.5 (2.0)	3

* Data is expressed as percent ± standard error.

TABLE III

Concentration of Each Form of Actin in Axoplasm

	Stable polymer*	Soluble polymer*	Monomer*	*n*
Single axon kinetics	27. ± 2.4 (0.38)	26.2 ± 3.5 (0.37)	46.8 ± 3.5 (0.66)	5
Ratio kinetics	25.3 ± 2.6 (0.35)	33.2 (0.47)	41.5 (0.58)	3
Phalloidin treatment	57.6 ± 2.2 (0.81)		42.4 ± 2.2 (0.59)	2

* Data is expressed as percent ± standard error.

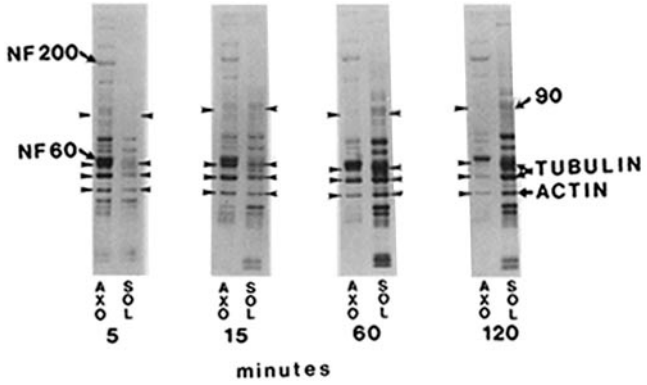

FIGURE 9 Ratio KEP: several gels showing protein elution. This figure illustrates representative samples at four time points in the ratio modification of the KEP. Each pair of gel columns contains the sample of axoplasm (*AXO*) and the soluble proteins (*SOL*) after a unique extraction time (5, 15, 60, and 120 min). Any protein may be compared in each pair from left to right to get an idea of its rate of elution. For example, the 90-kdalton band is only partially solubilized at 5 min but is almost completely extracted from the axoplasm by 60 min. NF proteins are not detected in the soluble column at any time.

and prepared for SDS PAGE.

Quantitative analysis of individual proteins in the two samples was carried out to obtain a ratio between the amount of protein extracted from the cylinder and the amount remaining in the cylinder at each time. Data were collected at time points ranging from 2–120 min. To minimize geometric differences between samples of axoplasm, all axons used in this analysis were between 550 and 650 μm in diameter and the diameters of extruded axoplasm were recorded. The axoplasm and samples of soluble protein were run on adjacent columns of SDS gels and stained with Coomassie Blue. Fig. 9 shows examples of preparations at 5, 15, 60, and 120 min after extrusion. Note that the NF proteins are not detected in the soluble fraction at any time.

Elution profiles were determined using analytical densitometry and are illustrated in Fig. 10, *a* and *b*. The shaded

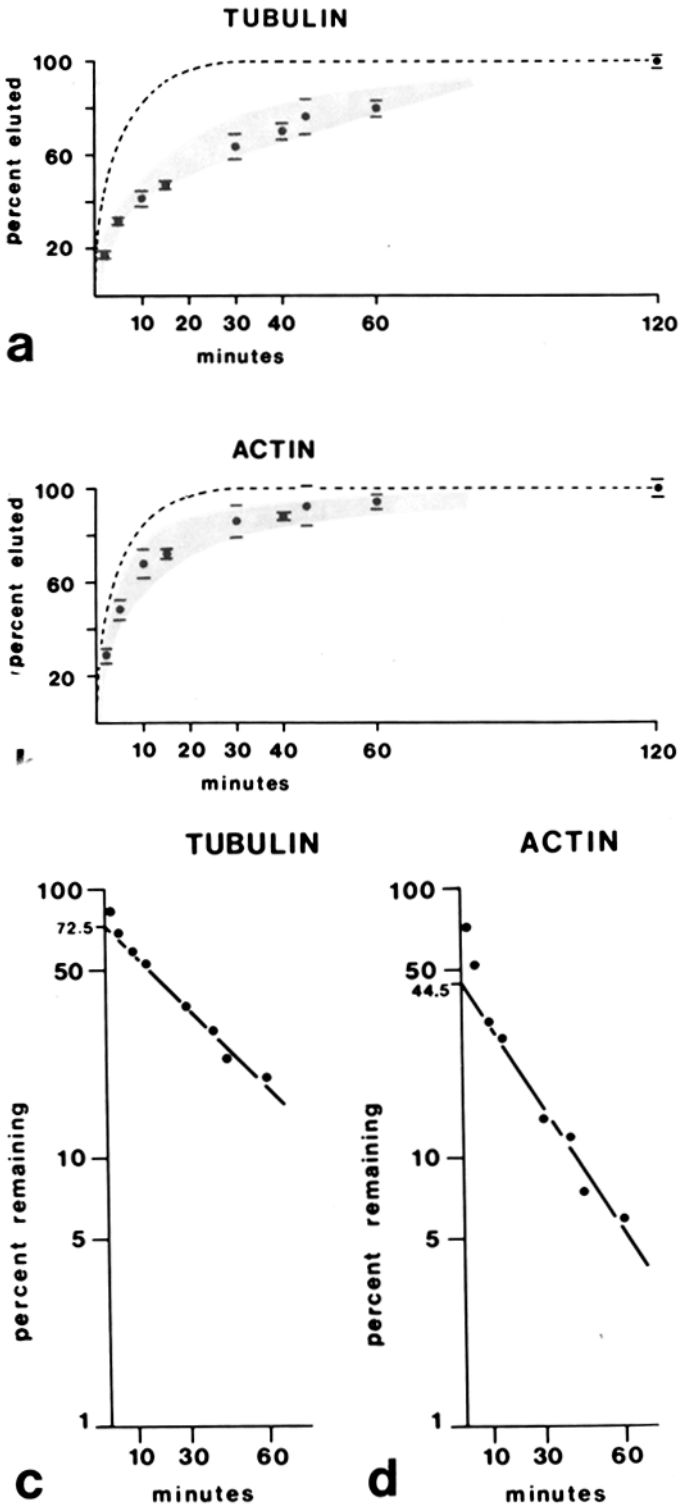

FIGURE 10 (*a* and *b*) Ratio KEP: elution profiles of tubulin and actin on cartesian axes. This figure shows the data means (filled circles) and standard error bars for the elution of tubulin and actin as measured by the ratio KEP. The shaded region is the 95% confidence envelope taken from the single axon KEP (see Fig. 7, *a* and *b*). The two methods clearly give similar results and both show that the elution of tubulin and actin is slowed when compared with theory (dashed line) for the diffusion of monomeric protein. (*c* and *d*) Ratio KEP: elution profiles of tubulin and actin on semilog axes. This figure shows the data means of Fig. 17 plotted on semilog axes. A value for the fraction of soluble protein which is dynamic polymer may be determined by extrapolating the linear regression line for the data at later times to the percent remaining axis at 0 time.

region in this figure represents the 95% confidence envelope taken from the previous (single axon KEP) experiments to facilitate the comparison of these protocols. The bars around each data point (filled circles) represent the standard error of the mean. It is clear that the ratio analysis data fall within the confidence envelope of the single axon KEP. Therefore, the two methods give similar results for the elution of tubulin and actin from axoplasm. The standard errors are, in general, greater in the ratio analysis than in the single axon KEP. This difference could result from the small variations in the diameter between samples of extruded axoplasm.

Fig. 10, *c* and *d* show the semi-log plots for the sample means of the ratio analysis for tubulin and actin. Linear regression was used to fit a line to the second component in a manner identical to that applied in the single axon KEP. The fraction of protein in the second component at the beginning of the experiment was determined by extrapolating the lines drawn through the second component to the percent remaining axis. The relative fraction of each protein in the first and second components was compared with that remaining stably associated with the axoplasm after 120 min. The sum of these three fractions correspond to the total amount of tubulin or actin in the cylinder of axoplasm at the beginning of the experiment. The results of this analysis are listed in Table II for tubulin and Table III for actin next to the heading "Ratio KEP". The measurements of the three components in both versions of the KEP are consistent. They show that a large fraction of the tubulin (58.8 ± 2.9%) and the actin (26.2 ± 3.5%) in axoplasm contributes to the second component (Tables II and III, under "soluble polymer").

Measurements of Cytoskeletal Protein Solubility Using Polymer Stabilizing Drugs

The single axon KEP and the ratio KEP are independent experiments that gave essentially equivalent results for the elution of tubulin and actin in axoplasm. However, because they both rely upon the same general model (the equilibration of a cylinder by diffusion) it would be useful to compare their results to measurements of tubulin and actin solubility using a completely different paradigm. The equilibrium model predicts that the tubulin and actin in the second component is polymerized in axoplasm. Consequently, we designed a study to investigate the effects of selected polymer stabilizing drugs on the solubilities of these cytoskeletal proteins.

Several drugs have recently been identified that stabilize either tubulin (MT) or actin polymers (MF) with some specificity. Taxol, a chemotherapeutic agent purified from plant *Taxus brevifolia*, stabilizes MT in vivo and in vitro (49, 50). MT which are polymerized in the absence of taxol are stabilized after only a few minutes of exposure to the drug (48). This result suggests that taxol binding sites are available in intact MT. Taxol reversibly stabilizes MT in living cells and inhibits cell migration and mitosis (50). Fig. 11 shows a comparison of axoplasm extracted in either buffer P (Fig. 10*a*) or buffer P containing 10 μM taxol (Fig. 11*b*). It is clear that substantially more tubulin is retained in the axoplasmic ghost when taxol is present (compare the G and S columns in each case). Electron microscopy of the "taxol ghost" reveals many MT although they are only rarely found when axoplasm is extracted in buffer alone (34). These MT account for the tubulin that remains in the taxol ghost. It is also important to note that a fraction of the tubulin in axoplasm is soluble despite the presence of taxol (in the right hand column *S* in Fig. 10*b*). It is likely that this fraction of the tubulin comes primarily from two sources. The majority is probably not included in MT and therefore is not subject to stabilization by taxol. The rest of the soluble tubulin could have come from MT which depolymerized in the first few minutes after extrusion, before taxol could diffuse into the axoplasm and stabilize the MT.

Next, taxol was applied in an experiment designed to measure the amounts of taxol-soluble, taxol-sensitive, and stably-polymerized tubulin in axoplasm. The soluble proteins of axoplasm were extracted in a bath of buffer P with taxol. Then, the axoplasm was transferred to a bath of buffer P without taxol and extracted until the stabilizing effects of taxol were reversed. During this second extraction, any MT which were initially stabilized by taxol should depolymerize. The proteins that remain insoluble after the axoplasm is extracted in taxol-free buffer should be the stable polymers of axoplasm.

Results of this type of taxol extraction experiment are illustrated in Fig. 12. Samples of axoplasm were extracted for a total of 125 min in two baths (5 and 120 min) with either buffer P (control) or buffer P + taxol (experiment). The gel containing the control sample shows that essentially all of the soluble tubulin is extracted in the first two baths. In the presence of taxol, in the gel on the right, much less tubulin is extracted. Then both samples of axoplasm were transferred

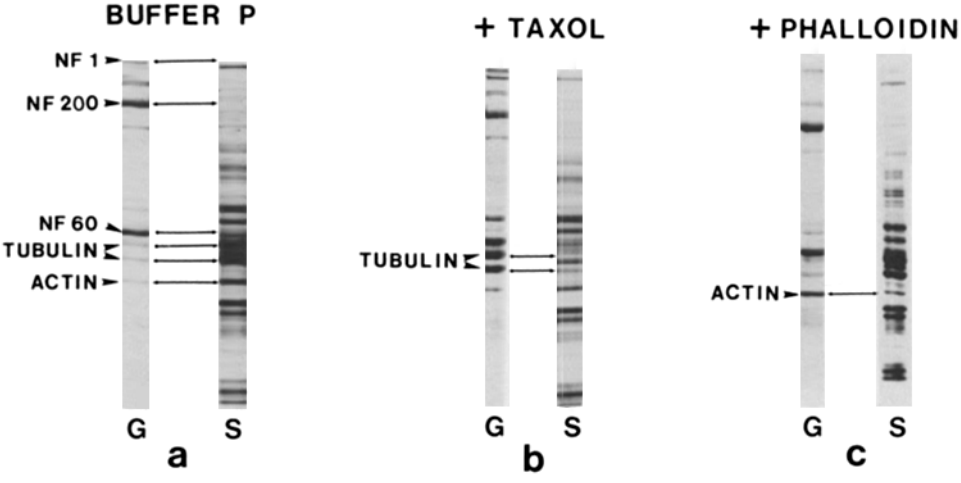

FIGURE 11 This figure illustrates the effects of taxol and phalloidin on the solubilities of axoplasmic proteins (3-h extractions). The gel columns labeled *a* show the insoluble ghost (*G*) proteins and the soluble (*S*) proteins when axoplasm is extracted in buffer P. The columns labeled *b* show a similar comparison when taxol (10 μM) is included in the buffer. Note that a significant fraction of the tubulin is rendered insoluble in this case. The gel columns labeled c show a similar experiment except that phalloidin (10 μM) was used. In this case a fraction of the actin is affected.

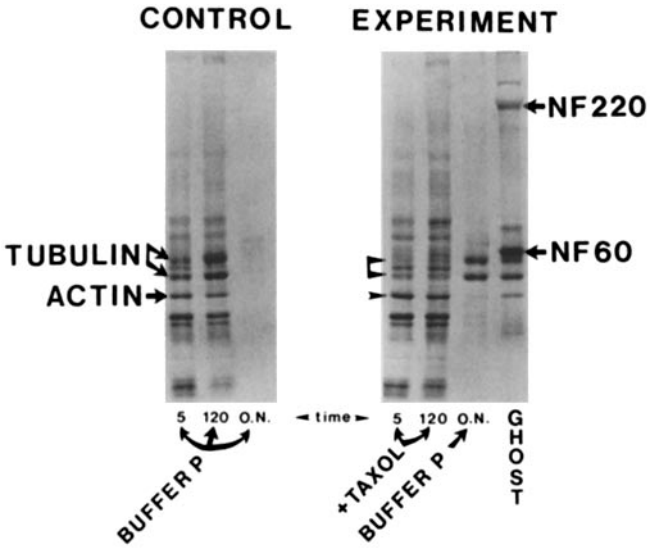

FIGURE 12 Taxol: used to measure three types of tubulin association in axoplasm. The gel on the left contains the soluble proteins that eluted after 5- and 120-min, and overnight (*O.N.*) extractions in buffer P. Note that protein elution is essentially complete after 120 min. The first two columns in the gel on the right shows the soluble proteins of axoplasm after 5 and 120 min of extraction in buffer P with taxol. Note the reduced amount of soluble tubulin as compared with the control whereas the solubility of actin is unaffected. The third column shows that the MT stabilizing effect of taxol is reversed if the axoplasm is transferred to a bath of buffer P without taxol and extracted overnight. The fourth column in the gel on the right contains the typical ghost proteins remaining at the end of this experiment.

into baths containing buffer P without taxol and extracted overnight. The control gel column is empty at this point because essentially all of the soluble protein was extracted from axoplasm in the first two baths. On the other hand, the sample of axoplasm that was treated with taxol contains tubulin which is extruded after the taxol is removed. Finally, the column on the far right contains the axoplasmic ghost from the taxol-treated sample with its typical complement of NF proteins, tubulin, and actin. This result supports the idea that a fraction of the soluble tubulin is polymerized as MT at the time of extrusion. Gels similar to the one in Fig. 12 were scanned with a densitometer and the amount of tubulin in each fraction was measured. These data are shown in Table II next to the heading "Taxol Treatment."

Another drug that alters cytoskeletal polymer stability is phalloidin, a bicyclic peptide toxin isolated from the mushroom *Amanita phalloides* (59). Phalloidin stabilizes the actin containing MF by binding directly to sites in the polymer (30). Although the details of Phalloidin-induced stabilization are not understood it may act by the allosteric modification of actin subunits or by cross-linking adjacent polypeptides in the MF polymer (59). In vivo, phalloidin stabilizes cytoplasmic actin and interferes with cell locomotion and growth (57). These results prompted the selection of phalloidin to measure the concentration of monomeric and polymerized actin in axoplasm.

In this experiment, a sample of axoplasm was extruded into buffer P containing phalloidin (10 μM) and extracted for 2 h. Fig. 11 illustrates the results of this experiment. The gel columns on the left (Fig. 10*a*) show the insoluble (*G*) and soluble (*S*) proteins when axoplasm is extracted in buffer P. When a sample of axoplasm is extracted in the presence of phalloidin much more actin is insoluble (compare the actin in the *G* and *S* columns in Fig. 11*c*. Gels with samples extracted in buffer P + phalloidin were scanned with a densitometer to measure the stabilized (polymer) and soluble monomer fractions of actin. These values are included in Table II next to the heading "Phalloidin Treatment." It was found that 41.1% of the actin in axoplasm is soluble in buffer P with phalloidin. On the other hand, the fraction of actin that is insoluble in phalloidin, 57.6%, is similar to the sum of the stable polymer and soluble polymer fractions found using the KEP.

DISCUSSION

The KEP Can Be Used To Distinguish Free Monomer From Polymer

Our results demonstrate that the KEP provides an effective model for studying the diffusibility of molecules in axoplasm. We found that the elution rate of two small molecules [^{3}H]leucine and ^{125}I was indistinguishable from that predicted by diffusion theory (Fig. 4). Previous studies have demonstrated that small molecules such as K^+ also diffuse freely in the axoplasm (13). Apparently, the cytoplasmic matrix of the axoplasm does not impede the diffusion of small molecules through the axoplasm. By contrast, the rate of elution of actin and tubulin were significantly different from the rate predicted by simple diffusion of the monomer. The retardation of the elution of these proteins from the axoplasm apparently reflects the association of some fraction of the proteins with the nondiffusible cytoskeleton. In the case, of tubulin and actin, this result can be readily explained, if a fraction of these proteins is in the form of soluble polymer.

To distinguish proteins that are in the form of diffusible monomer from those in the form of soluble polymer, the elution rate for monomer must be measurably different from the rate of the depolymerization reaction. This appears to be true for the molecules that we have measured in squid axoplasm. The elution profiles for both actin and tubulin have two components that are easily resolved from one another. When the first component is extracted from the data by the process of exponential peeling, it corresponds to the rate predicted for the free diffusion of a protein from a cylinder of water. Apparently the cytomatrix of the axoplasm does not impede the diffusion of small molecules or monomeric proteins such as tubulin and actin sufficiently to be detected by the KEP. Electron microscopic analyses of the axon indicate that the mesh-size of the axoplasmic matrix is considerably greater than the size of either actin or tubulin (33, 35).

The Second Component of Elution Represents the Disassembly of Soluble Polymers

The slope of the second component of elution differs from that of the first component by an order of magnitude. Clearly, the rate of the second component is limited by some process other than diffusion. We propose that the limiting process of the second component is the disassembly reaction of soluble polymers. Our observations indicate that the concentration of monomer drops very rapidly after the axoplasm is placed into the buffer. The axoplasmic concentration of monomer drops by more than one half during the first 5 min of initiating

the KEP (Figs. 8 and 10). Under these conditions any axoplasmic MT or MF that has one or both ends free to exchange subunits with the monomer pool should disassemble. If the rate of disassembly is relatively slow as compared with the rate of diffusion of monomer from the axoplasm, then the slope of the second component should reflect the rate of the dissociation reaction.

We can analyze this possibility by comparing the rate of the second component with the rates of polymer disassembly determined for purified components in vitro (20, 21). In vitro measurements have been obtained for MT by a rapid dilution technique that is analogous to the KEP. MT disassembly is a first order reaction for long polymers and the slope of the disassembly curve represents a measure of the dissociation rate for MT. The second component of elution from axoplasm is also a first order reaction (correlation coefficient = 0.995). Therefore, we can compare the rate of dissociation estimated from the second component of elution in our experiments with the rate measured in vitro. We obtain a dissociation rate of 61%/h for tubulin from the soluble MT, which is in the range of 35–160%/h reported by Margolis and Wilson for MT disassembly in the presence of 1 mM ATP (this is equivalent to the ATP concentration in our buffer). Our estimates of the dissociation rate of actin from soluble MF in axoplasm are 62%/h which is also consistent with analyses of purified MF in vitro (44). The similarity of these results support our proposal that the second component of elution represents the dissociation of soluble polymers and that the slope of the second component is a measure of the rate of the off reaction for axonal MT and MF which are in equilibrium with the monomer pool.

Monomer-Polymer Equilibria Determined with Taxol and Phalloidin

More direct support for the hypotheses that the second component of elution corresponds directly to the depolymerization of soluble MT or MF is provided by the experimental results with taxol and phalloidin (50, 59). We found that a fraction of the tubulin and actin that elutes from the axoplasm was rendered insoluble by these drugs. Electron microscopic analyses demonstrate that taxol acts on the MT in the squid axoplasm (J. R. Morris, R. J. Lasek, and A. Hodge; unpublished). Thus, our results confirm previous studies that taxol and phalloidin act selectively on MT and MF, respectively.

In the experiments with taxol the amount of monomer was calculated from the total amount of tubulin that eluted from the axoplasm. It was possible to estimate the fraction of tubulin that was present in MT that were selectively stabilized by taxol, because taxol binds reversibly to MT (50). Thus, the taxol-stabilized MT could be removed from the axoplasm by simply removing the taxol from the buffer (Fig. 12). Estimates of monomer, polymer, and stable polymer by this method were similar to those obtained with the KEP (Table II). However, the monomer concentration determined by the taxol method was higher than that determined by the KEP, and the soluble polymer concentration was proportionally lower. This may be explained by the time it takes for taxol to act in the MT when it is added to axoplasm. To avoid the possibility of driving excess polymerization of MT with taxol, we did not preincubate the giant axon in taxol prior to extrusion. Instead axoplasm was extruded into buffer containing taxol. Thus, the slightly higher values for the monomeric form of tubulin in the taxol experiments may result from the interval required for taxol to take effect after it was introduced into the axoplasmic cylinders. If some of the MT began to depolymerize before the taxol took effect then this depolymerization would contribute to the total amount of tubulin that entered the buffer and was considered monomeric.

The results obtained for MF using phalloidin were very similar to those obtained with the KEP, but phalloidin was not reversible and it was not possible to separate soluble polymer from stable polymer (Table III). The similarity between the pharmacological results and those from the KEP experiments indicate that either of these methods can be used to estimate the relative fraction of monomer and soluble polymer in axoplasm and therefore to obtain a measure of the monomer-polymer equilibrium for MT and MF in the axon. Although the KEP appears to be limited to very large axons such as the squid giant axon, it may be possible to extend the use of taxol and phalloidin to smaller axons by using detergents to permeabilize the plasma membrane (53).

Monomer-Polymer Equilibria Differ In Vitro and In Vivo

The measurements of (soluble) polymer and monomer obtained using the KEP provide one basis for estimating the steady state equilibrium for axoplasm in vivo because they were obtained under conditions that simulate those inside of the axon. For comparison, Table IV lists a number of representative examples of the equilibria that occur in vitro when the concentration of total actin or tubulin in the solution was the same as that found in axoplasm (soluble polymer plus monomer). It is notable that the relative proportion of monomeric tubulin and actin in axoplasm is larger than that obtained in vitro. For tubulin the difference is about a factor of 3 (1.47 mg/ml as compared to 0.4 mg/ml) and for actin the difference is about a factor of 2 (0.66 mg/ml as compared with 0.28 mg/ml). Similar observations have been made for the monomer-polymer ratios in neuroblastoma cells (39). The differences in the results in vivo and in vitro suggest that factors are present in the cell that act to inhibit the polymerization of tubulin and actin.

There are a number of possible mechanisms by which polymerization could be controlled in axoplasm. Excess polymerization could be limited by restrictions on certain factors that promote the polymerization of MT or MF (36, 38, 40, 55). For example, factors such as microtubule-associated proteins can act to raise the critical concentration of tubulin required for polymerization (36, 37). We have identified two high molecular weight proteins that may be microtubule-

TABLE IV

Comparison of Monomer-Polymer Equilibria for Tubulin and Actin with Other Results In Vitro

	Soluble polymer	Monomer
	mg/ml	*mg/ml*
Tubulin		
Single axon KEP	3.29	1.47
	4.4*	0.4*
Actin		
Single axon KEP	0.37	0.66
	0.82‡	0.28‡

* Olmstead et al. (38).
‡ Wegner and Engel (55).

associated proteins because they are selectively retained within the axoplasm when it is treated with taxol but elute when the taxol is removed (J. R. Morris and R. J. Lasek, unpublished results). It will be interesting to determine the relative stoichiometry of these proteins to tubulin if they are shown to be microtubule-associated proteins by additional criteria.

Another possible mechanism for regulating MT polymerization in axoplasm is that some of the unpolymerized tubulin or actin may be bound to regulating polypeptides or other molecules that inhibit polymerization by lowering the concentration of effective monomer in axoplasm. Several such factors have been identified in the soluble fraction of homogenized tissue (7, 14, 31, 52). Some of these factors are relatively small proteins and would not have had a large enough effect on the rate of diffusion of monomeric tubulin or actin to be detected by the KEP. Yet, another possible in vivo regulatory mechanism is that tubulin and actin are post-translationally modified in ways that directly influence their ability to polymerize. However, we did not observe any differences in the isoelectric point of either axoplasmic tubulin or actin when we compared it with actin and tubulin from whole brain. More information will be required to determine which of these mechanisms regulates the monomer-polymer equilibria in axons.

In Vivo Monomer-Polymer Equilibria and Axonal Transport of the Cytoskeleton

To put our chemical kinetic data in its proper biological context, it is important to recall that the mature nongrowing axon is a steady state system. Cytoskeletal proteins are continually transported through the axon from the cell body, where they are synthesized, toward the axon terminal where they appear to be selectively degraded (25, 27). The cytoskeletal elements move at a rate of 1–5 mm/d from the cell body toward the axon terminal (27, 29). Apparently, very little degradation of the proteins occurs in transit and only a small amount of cytoskeletal protein is left behind by axonal transport (25).

One model of axonal transport holds that cytoskeletal proteins are actively transported through the axon only when they are in the form of polymer (for review see 28, 29); and in this context, it is interesting that the squid giant axon contains both stable and soluble polymers (Tables II and III). We can not be certain that all of the stable tubulin is in the form of polymer and it is possible that some may be in another insoluble form. However, a significant fraction of this tubulin represents stably polymerized MT, because stable MT were observed in the extracted axoplasm (35).

Stable and soluble polymer may both be present in the same population of MT. That is, individual MT may contain a stable region that cannot disassemble but that can support assembly. MT that have both a stable region and a soluble region will confer interesting properties on the transported cytoskeleton. For example, the stable region within the MT prevents treadmilling of tubulin through the MT because the disassembly reaction is blocked when the stable region reaches either the plus or minus end of the microtubule. In fact, MT with a stable minus end would act to eliminate MT that have both ends free and can treadmill (23). That is, the stable polymers can act as nucleating sites that inhibit the random and spontaneous polymerization of MT in the axon (23). Thus, if the stable polymers can support assembly the mixed polymers will predominate in the axon and will represent the principal component of axonally transported polymer.

Monomer Equilibria Influence the Stability and Plasticity of Neuronal Structure

The axonal cytoskeletal proteins are renewed at a relatively slow rate (1–5 mm/d). In long axons, it can take years for proteins to travel from the cell body to the distal reaches of the axon (25, 27). The stable MT and MF in the axon may provide the necessary stability to buffer the cytoskeleton against irreversible disruption as these proteins make their way slowly along the axon. This stability is required both to maintain the external shape of the axon and to provide the microstructure for the directed movement of membrane traffic within the axon (4). In fact, during the development of the axon the neuronal cytoskeleton may be converted to a more stable form. For example, the relative amount of polymerized tubulin increases during neurite extension in developing neurons and neuroblastoma cells (1, 39). Some axons may develop extremely stable cytoskeletons. For example, >60% of the axonally transported tubulin in mammalian retinal ganglion cells appears to be in the form of stable MT (3).

Although the axonal cytoskeletal system must provide stability for the axon, it must also be capable of change, because axons exhibit marked plasticity (11, 28). For example, many axons regenerate when they are injured. In long axons, such as the squid giant axon, new polymers in a regenerating sprout are formed from the existing pools of cytoskeletal proteins that are present in the axon (17, 27). That is, reorganization of the axonal cytoskeleton does not require the participation of newly synthesized proteins from the cell body. Our analyses indicate that the squid giant axon contains an abundance of tubulin and actin that could be used for the polymerization of new microtubules and microfilaments during regeneration. More than 80% of the tubulin and 75% of the actin in the giant axon is in the form of soluble polymer or monomer (Tables II and III). Subunits could be drawn for assembly directly from the free monomer pool or they could by recycled from the soluble polymers. For example, during the initial (injury) phase of regeneration, the axon is permeable to extracellular ions, including Ca^{++}. The entry of these ions could promote the disassembly of MT and provide additional subunits for the polymerization of new polymers when the axon regains its normal permeability properties. This represents one of the many ways that subunits in equilibrium between the monomer pool and soluble polymers could be used for cytoskeletal reorganization.

These observations lead us to propose that the monomer-polymer equilibria in the squid giant axon are set to provide a balance between the requirements for stability and plasticity. More specifically, stable polymers may maintain the structural pattern within the cytoskeleton as it slowly makes its way from the cell body to the synaptic terminal. These stable polymers include the neurofilaments (28, 29, 35), stable microtubules (3), and stable microfilaments. To counterbalance these stabilizing influences the cytoskeletal system of the axon has a vast source of tubulin and actin in dynamic equilibrium between the monomer pool and the soluble polymers. This reservoir of subunits may contribute to the remarkable ability of the axon to undergo morphological changes at any point along its length without the direct participation of protein synthesis.

TABLE V

Diffusion Coefficients

Diffusing species	Diffusion coefficient	Reference
	cm^2/s	
^{125}I	9.92×10^{-6}	Einstein equation
[^{3}H]leucine	1.06×10^{-5}	Weast (54)
Tubulin dimer	4.91×10^{-7}	Svedberg equation; Borisy
G-actin	5.28×10^{-7}	Weast (54)

APPENDIX I

Mathematic Theory For the Kinetic Equilibration Paradigm

The extruded axoplasm is treated as an infinitely long uniform cylinder that is equilibrating by diffusion, with an infinitely large bath. The solution of Fick's Diffusion Equation for this case is called the Fractional Equilibration Equation for a Cylinder and is published in both Hill or Kotyk and Janecek (15, 24). The solution is presented as an infinite series:

where,

F = the fraction of diffusant remaining in the cylinder;
M_t = the concentration of diffusant eluted at time t;
M_o = the concentration of diffusant at time zero;
D = the diffusion coefficient (square centimeters per second);
t = time in seconds;
r = radius of cylinder in centimeters;
u_x = the zeroes of the Bessel Function Jo; the first eight are:
$u_1 = 2.4048$; $u_2 = 5.5021$; $u_3 = 8.6537$;
$u_4 = 11.7915$; $u_5 = 14.931$; $u_6 = 18.071$;
$u_7 = 21.212$; $u_8 = 24.352$.

The diffusion coefficients that were used in the Equilibration Equation are shown in Table V.

The authors would like to express their appreciation to Drs. Michael Katz and Scott Brady for their helpful suggestions during the preparation of this manuscript.

This work was supported by a grants from the National Institutes of Health AG 00084 and NS15731 to R. J. Lasek and NRSA Postdoctoral Training Award NS07118 to J. R. Morris.

Received for publication 26 April 1983, and in revised form 28 December 1983.

REFERENCES

1. Black, M. M., J. M. Cochran, and J. T. Kurdyla. 1983. Solubility properties of neuronal tubulin. Evidence for labile and stable microtubules. *J. Neurochem.* In press.
2. Blikstad, I., F. Markey, L. Carlsson, T. Persson, and U. Lindberg. 1978. Selective assay of monomeric and filamentous actin in cell extracts, using inhibition of deoxyribonuclease 1. Call. 15:935–943.
3. Brady, S. T. 1981. Biochemical and solubility properties of axonal tubulin. *J. Cell Biol.* 91:333*a*. (Abstr.)
4. Brady, S. T., R. J. Lasek, and R. D. Allen. 1982. Fast axonal transport in extruded axoplasm from squid giant axon. *Science (Wash. DC)* 218:1129–1131.
5. Brinkley, B. R., C. L. Miller, J. W. Fuseler, D. A. Pepper, and L. J. Wible. 1978. Cytoskeletal changes in cell transformation to malignancy. *In* Cell Differentiation and Neoplasia. G. F. Saunders, editor. Raven Press, New York. 419–450.
6. Brinkley, B. R., C. M. Cox, D. A. Pepper, L. Wible, S. L. Brenner, and R. L. Pardue. 1981. Tubulin assembly sites and the organization of cytoplasmic microtubules in cultured mammalian cells. *J. Cell Biol.* 90:8–16.
7. Carlsson, L., L. E. Nystrom, I. Sundkvist, F. Markey, and U. Lindberg. 1977. Actin polymerizability is influenced by profilin, a low molecular weight protein in non-muscle cells. *J. Mol. Biol.* 115:465–483.
8. Deffner, G. J., and R. E. Hafter. 1960. Chemical investigations of the giant nerve fibers of the squid. *Biochem. Biophys. Acta.* 42:200–205.
9. Deffner, G. J. 1961. The dialyzable free organic constituents of squid blood; a comparison with nerve axoplasm. *Biochem. Biophys. Acta.* 47:378–388.
10. Fine, R. E., and L. Taylor. 1976. Decreased actin and tubulin synthesis in 3T3 cells after transformation by SV40 virus. *Exp. Cell Res.* 102:162–168.
11. Friede, R. L., and R. Bischhausen. 1980. The fine structure of stumps of transected nerve fibers in subserial sections. *J. Neurol. Sci.* 44:181–203.
12. Friedman, L. 1930. Structure of agar gels from studies of diffusion. *J. Am. Chem. Soc.* 52:1311–1314.
13. Gilbert, D. S. 1975. Axoplasm architecture and physical properties as seen in the Myxicola giant axon. *J. Physiol.* 253:257–301.
14. Harris, H. E., and A. G. Weeds. 1978. Platelet actin: sub-cellular distribution and association with profilin. *FEBS (Fed. Eur. Biol. Soc.) Lett.* 90:84–88.
15. Hill, A. V. 1928. The diffusion of oxygen and lactic acid through tissues. *Proc. R. Soc. Lond. B. Biol. Sci.* 104:39–96.
16. Hill, T. L., and M. W. Kirschner. 1982. Bioenergetics and kinetics of microtubule and actin filament assembly-disassembly. *Int. Rev. Cytol.* 78:1–125.
17. Hoffman, P. N., and R. J. Lasek. 1980. Axonal transport of the cytoskeleton in regenerating motor neurons: constancy and change. *Br. Res.* 202:317–333.
18. Huneeus, F. C., and P. F. Davison. 1970. Fibrillar proteins from squid axons. I. Neurofilament protein. *J. Mol. Biol.* 52:415–428.
19. Inoue. S. 1964. Organization and function of the mitotic spindle. *In* Primitive Motile Systems in Biology. R. D. Allen and N. Kamiya, editors. Academic Press Inc., New York. 549–598.
20. Karr, T. L., and D. L. Purich. 1979. A microtubule assembly/disassembly model based on drug effects and depolymerization kinetics after rapid dilution. *J. Biol. Chem.* 254:10885–10888.
21. Karr, T. L., D. Kristofferson, and D. L. Purich. 1980. Mechanism of microtubule depolymerization. *J. Biol. Chem.* 255:8560–8566.
22. Kirschner, M. W. 1978. Microtubule assembly and nucleation. *Int. Rev. Cytol.* 54:1–69.
23. Kirschner, M. W. 1980. Implications of treadmilling for the stability and polarity of actin and tubulin polymers in vivo. *J. Cell. Biol.* 86:330–334.
24. Kotya, A., and K. Janacel. 1970. Cell membrane transport. Plenum Press, Inc. New York. 29–41.
25. Lasek, R. J., and P. N. Hoffman. 1976. The neuronal cytoskeleton, axonal transport and axonal growth. *In* Cell Motility. Cold Spring Harbor Symposium NRP. 1021–1049.
26. Lasek, R. J., H. Gainer, and J. L. Barker. 1977. Cell-to-cell transfer of glial proteins to the squid giant axon. *J. Cell Biol.* 74:501–523.
27. Lasek, R. J. 1981. The dynamic ordering of the neuronal cytoskeleton. *Neurosci. Res. Prog. Bull.* 19:7–32.
28. Lasek, R. J., and J. R. Morris. 1982. The microtubule-neurofilament network: the balance between plasticity and stability in the nervous system. *In* Biological Function of Microtubules and Related Structures. H. Sakai, editor. Academic Press, Inc., Tokyo.
29. Lasek, R. J., I. G. McQuarrie, and S. T. Brady. 1983. *In* Biological Structures and Coupled Flows. A. Silverberg, editor. Balakon Press, Rehovot, Israel. In press.
30. Lengsfeld, A. M., I. Low, T. Wieland, P. Dancker, and W. Hasselbach. 1974. Interaction of phalloidin with actin. *Proc. Natl. Acad. Sci. USA.* 71:2803–2807.
31. Lockwood, A. H. 1979. Molecules in mammalian brain that interact with the colchicine site on tubulin. *Proc. Natl. Acad. Sci. USA.* 76:1184–1188.
32. Merriam, R. W., and T. G. Clark. 1978. Actin in xenopus oocytes II. Intracellular distribution and polymerizability. *J. Cell Biol.* 77:439–447.
33. Metuzals, J., A. Hodge, R. J. Lasek, and I. R. Kaiserman-Abramof. 1983. Neurofilamentous network and filamentous matrix preserved and isolated by different techniques from squid giant axon. *Cell Tissue Res.* 228:415–432.
34. Morris J. R., A. Hodge, and R. J. Lasek. 1981. The microtubule network in the squid giant axon. *Biol. Bull.*
35. Morris, J. R., and R. J. Lasek. 1982. Stable polymers of the axonal cytoskeleton. The axoplasmic ghost. *J. Cell Biol.* 92:192–198.
36. Murphy, D. B., and G. G. Borisy. 1975. Association of high molecular weight proteins with microtubules and their role in microtubule assembly in vitro. *Proc. Natl. Acad. Sci. USA.* 72:2696–2700.
37. Murphy, D. B., K. A. Johnson, and G. G. Borisy. 1977. Role of tubulin-associated proteins in microtubule nucleation and elongation. *J. Mol. Biol.* 117:33–52.
38. Olmsted, J. B., J. M. Marcum, K. A. Johnson, C. Allen, and G. G. Borisy. 1974. Microtubule assembly: some possible regulatory mechanisms. *J. Supramol. Struct.* 2:429–450.
39. Olmsted, J. B. 1981. Tubulin pools in differentiating neuroblastoma cells. *J. Cell Biol.* 89:418–423.
40. Oosawa, F., and M. Kasai. 1962. Theory of linear and helical aggregations of macromolecules. *J. Mol. Biol.* 4:10–21.
41. Otto, J. J., and J. Bryan. 1981. The incorporation of actin and fascin into the cytoskeleton of filopodial sea urchin coelomocytes. *Cell Motility.* 1:179–192.
42. Pipeleers, D. G., M. A. Pipeleers-Marichal, and D. M. Kipnis. 1977. Physiological regulation of total tubulin and polymerized tubulin in tissues. *J. Cell Biol.* 74:351–357.
43. Pipeleers, D. G., M. A. Pipeleers-Marichal, P. Sherline, and D. M. Kipnis. 1977. A sensitive method for measuring polymerized and depolymerized forms of tubulin in tissues. *J. Cell Biol.* 74:341–350.
44. Pollard, T. D., and M. S. Mooseker. 1981. Direct measurement of actin polymerization rate constants by electron microscopy of actin filaments nucleated by isolated microvillus cores. *J. Cell Biol.* 88:654–659.
45. Rubin, R. W., and G. D. Weiss. 1975. Direct biochemical measurements of microtubule assembly and disassembly in chinese hamster ovary cells. *J. Cell Biol.* 64:42–53.
46. Rubin, R. W., R. H. Warren, D. S. Lukeman, and E. Clements. 1978. Actin content and organization in normal and transformed cells in culture. *J. Cell Biol.* 78:28–35.
47. Rubinow, S. 1975. Introduction to Mathematical Biology. John Wiley and Sons, New York.
48. Schiff, P. B., J. Fant, and S. B. Horwitz. 1979. Promotion of microtubule assembly in vitro. *Taxol Nature.* 277:665–667.
49. Schiff, P. B., and S. B. Horwitz. 1980. Tubulin: a target for chemotherapeutic agents. *In* Molecular Action and Targets for Cancer Chemotherapeutic Agents. Academic Press. 483–507.
50. Schiff, P. B., and S. B. Horwitz. 1980. Taxol stabilizes microtubules in mouse fibroblast cells. *Proc. Natl. Acad. Sci. USA.* 77:1561–1565.
51. Schliwa, M., and U. Euteneuer. 1978. Quantitative analysis of the microtubule system in isolated fish melanophores. *J. Supramol. Struct.* 8:177–190.
52. Sherline, P., and K. Shiavone. 1977. Immunofluorescence localization of proteins of high molecular weight along intracellular microtubules. *Science (Wash. DC).* 198:1083–1040.
53. Vallee, R. B. 1982. A taxol-dependent procedure for the isolation of microtubules and microtubule-associated proteins (MAPs). *J. Cell Biol.* 92:435–442.
54. Weast, R. C. 1980. CRC Handbook of chemistry and physics. 61st. Edition. *CRC Press, Inc,* Florida.
55. Wegner, A., and J. Engel. 1975. Kinetics of the cooperative association of actin to actin filaments. *Biophys. Chem.* 3:215–225.
56. Wegner, A. 1976. Head to tail polymerization of actin. *J. Mol. Biol.* 108:139–150.
57. Wehland, J., M. Osborn, and K. Weber. 1977. Phalloidin-induced actin polymerization in the cytoplasm of cultured cells interferes with cell locomotion and growth. *Proc. Natl. Acad. Sci. USA.* 74:5613–5617.
58. Weisenberg, R. C. 1972. Changes in the organization of tubulin during meiosis in the eggs of the surf clam, spisula solidissima. *J. Cell Biol.* 54:266–278.
59. Wieland, T. 1977. Modification of actins by phallotoxins. *Naturwissenchaften.* 64:303–309.